Robotica: (2020) volume 38, pp. 29–47. © Cambridge University Press 2019
doi:10.1017/S0263574719000456

Nonlinear Optimal Control for the Wheeled Inverted Pendulum System

G. Rigatos†*, K. Busawon‡, J. Pomares¶ and M. Abbaszadeh§

†*Unit of Industrial Automation, Industrial Systems Institute, Rion, Patras 26504, Greece*
‡*Nonlinear Dynamics Group, University of Northumbria, Newcastle NE1 8ST, UK.*
E-mail: krishna.busawon@northumbria.ac.uk
¶*Department of Systems Engineering, University of Alicante, 03080 Alicante, Spain.*
E-mail: jpomares@ua.es
§*GE Global Research, General Electric, Niskayuna, NY, 12309, USA.*
E-mail: masouda@ualberta.ca

(Accepted March 9, 2019. First published online: April 16, 2019)

SUMMARY
The article proposes a nonlinear optimal control method for the model of the wheeled inverted pendulum (WIP). This is a difficult control and robotics problem due to the system's strong nonlinearities and due to its underactuation. First, the dynamic model of the WIP undergoes approximate linearization around a temporary operating point which is recomputed at each time step of the control method. The linearization procedure makes use of Taylor series expansion and of the computation of the associated Jacobian matrices. For the linearized model of the wheeled pendulum, an optimal (*H*-infinity) feedback controller is developed. The controller's gain is computed through the repetitive solution of an algebraic Riccati equation at each iteration of the control algorithm. The global asymptotic stability properties of the control method are proven through Lyapunov analysis. Finally, by using the *H*-infinity Kalman Filter as a robust state estimator, the implementation of a state estimation-based control scheme becomes also possible.

KEYWORDS: Wheeled inverted pendulum; Nonlinear optimal control; *H*-infinity control; Approximate linearization; Taylor series expansion; Jacobian matrices; Riccati equation; Lyapunov analysis; Global stability.

1. Introduction

The problem of feedback control and stabilization of the wheeled inverted pendulum (WIP) is a nontrivial one due to the model's nonlinearities and underactuation.[1,2] Actually, one can use only two control inputs (wheels' torques) so as to control a system of more degrees of freedom. This control problem is of interest for the area of robotics because such a type of two-wheeled vehicles can be used for the transportation of humans and loads without the space and maneuvering limitations exhibited by four-wheel vehicles.[3–6] Previous attempts to solve this problem have been based primarily on global linearization control method and state-space transformation approaches.[7–10] However, one can find also several results based on approximate linearization techniques.[11–15] Additionally, one can note results relying on Lyapunov stability theory methods, as in the case of model-free adaptive control approaches.[16–22] In this article, to solve the control problem for the WIP, the system's dynamic model is first written in an affine-in-the-input form. For this latter description, a nonlinear optimal controller is developed.[23–25]

The dynamic model of the wheeled pendulum undergoes approximate linearization around a temporary operating point which is updated at each time step of the control method. The linearization

* Corresponding author. E-mail: grigat@ieee.org

point consists of the system's state vector and of the last control input that was exerted on it. The linearization procedure makes use of first-order Taylor series expansion of the system's dynamic model and requires the computation of the associated Jacobian matrices. The modelling error which is due to truncation of higher-order terms in the approximate linearization is considered to be a perturbation which is compensated by the robustness of the control algorithm. For the approximately linearized state-space description, an optimal (*H*-infinity) feedback controller is designed.[26–29]

The developed *H*-infinity controller stands for the solution of the optimal control problem for the WIP, under model disturbances and external perturbations. Actually, it represents the solution of a min–max differential game, in which the controller tries to minimize a quadratic cost function related with the state vector's tracking error, whereas the model uncertainty and external disturbances terms try to maximize this cost function.[30,31] For the computation of the controller's feedback gain, an algebraic Riccati equation has to be solved at each iteration of the control algorithm. The stability of the control method is proven through Lyapunov analysis. First, it is shown that the control loop satisfies the *H*-infinity tracking performance criterion, which signifies elevated robustness against modelling errors and external perturbations. Moreover, under moderate conditions the control loop is globally asymptotically stable. Additionally, to implement observer-based control for the model of the WIP, the *H*-infinity Kalman Filter is used as a robust state estimator.[32,33]

The structure of the article is as follows: in Section 2, the dynamic model of the WIP is analyzed and a description about it in an affine-in-the-input form is obtained. In Section 3, approximate linearization is performed on the dynamic model of the WIP using Taylor series expansion and the computation of the associated Jacobian matrices. In Section 4, the nonlinear optimal (*H*-infinity) control problem is formulated for the model of the WIP and a solution about it is introduced. In Section 5, the stability properties of the *H*-infinity control scheme are analyzed with the use of the Lyapunov method. In Section 6, state estimation-based control is proposed for the WIP after introducing the *H*-infinity Kalman Filter as a robust state estimator. In Section 7, the tracking performance of the control method is evaluated through simulation experiments. Finally, in Section 8, concluding remarks are stated.

2. Dynamic Model of the WIP

The WIP is a complex electromechanical system exhibiting both non-holonomic behavior and underactuation. It consists of a vertical body and of two co-axial driven wheels. The system is underactuated because it has less degrees of freedom than its control inputs. Moreover, the system is subject to non-holonomic constrains which are due to the pure rolling of the vehicle.[34–37] The WIP can find applications in the transportation of humans and products, while significant use of it is related with warehouse management. Thanks to its capacity for dexterous maneuvering and the simplicity in its production, the use of WIP in industrial-type applications is rapidly deploying.[38–40] A WIP exhibits several advantages comparing to automatic ground vehicles (AGVs). It has better maneuverability in flat surfaces and a self-balancing system which allows for carrying loads despite its small base size. Actually, it can carry a higher payload for the same base size of an AGV. Besides, WIP-type robots can move faster, with higher efficiency and with a simpler mechanism design than biped robots.

The diagram of the WIP is depicted in Fig. 1. The following reference frames are defined: $X_0Y_0Z_0$ which is the inertial reference frame, $X_1Y_1Z_1$ which is the body-fixed reference frame with axis O_1Y_1 to coincide with the wheels' axis of the vehicle, and $X_2Y_2Z_2$ which is the pendulum-fixed reference frame with axis O_2Z_2 to coincide with the pendulum's (pole's) axis.

The state variables of the WIP are: ψ which denotes the turn angle of the wheels' axis, θ which denotes the turn angle of the pendulum, and α which denotes the heading angle of the two-wheels vehicle. The dynamic model of the wheeled mobile robot can be obtained with the use of Euler–Lagrange analysis.[41,42] By defining the state vector of the WIP as $q = [\psi, \theta, \alpha]^T$, its dynamic model is written initially in the following state-space form:[1,2]

$$M(q)\ddot{q} + N(q, \dot{q}) + O(\dot{q}) = \tau \tag{1}$$

where $M(q)$ is the inertia matrix given by

$$M(q) = \begin{pmatrix} m_{11} & m_{12}cos(\theta) & 0 \\ m_{12}cos(\theta) & m_{22} & 0 \\ 0 & 0 & I_{bl}sin^2(\theta) + m_{33} \end{pmatrix} \tag{2}$$

https://doi.org/10.1017/S0263574719000456 Published online by Cambridge University Press

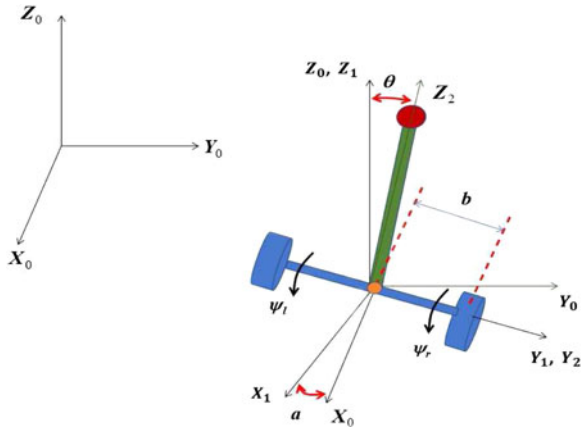

Fig. 1. Diagram of the WIP.

while the Coriolis and centrifugal terms matrix is given by

$$C(q, \dot{q}) = N(q, \dot{q}) + O(q) \tag{3}$$

where

$$N(q, \dot{q}) = \begin{pmatrix} -m_{12} sin(\theta)(\dot{\theta} + \dot{\alpha}^2) \\ -I_{bl} sin(\theta) cos(\theta)\dot{\alpha}^2 - G_b sin(\theta) \\ 2I_{bl} sin(\theta) cos(\theta)\dot{\theta}\dot{\alpha} + m_{12} sin(\theta)\dot{\psi}\dot{\alpha} \end{pmatrix} \tag{4}$$

$$O(q) = \begin{pmatrix} 2D_w\dot{\psi} - 2D_b(\dot{\theta} - \dot{\psi}) \\ 2D_b(\dot{\theta} - \dot{\psi}) \\ \frac{2b^2}{r^2}(D_b + D_w)\dot{\alpha} \end{pmatrix} \tag{5}$$

The main parameters of the model are: u_r and u_l are the torques of the right and left wheel, respectively, m_b and m_w are the masses of the body of the vehicle and of each one of its wheels, respectively, I_{bl} which is the moment of inertia of the pendulum around the y axis, I_{bz} which is the moment of inertia of the pendulum around the z axis, I_{bx} which is the moment of inertia of the wheel around its axis, I_{wa} and I_{wd} are the moments of inertia of the wheel around its axis and diameter, respectively, l which is the distance between the center of the wheels' axis and the center of gravity of the pendulum, r which is the radius of the wheel, $2b$ which is the length of the wheels' axis, D_b which is the viscous resistance of the driving system, and D_w which is the viscous resistance of the ground.[1,2]

In particular, the main parameters of the dynamic model of the WIP are defined as follows:

$$\begin{aligned} \psi &= \frac{1}{2}(\psi_l + \psi_r) \\ m_{11} &= (m_b + 2m_w)r^2 + 2I_{wa} \\ m_{12} &= m_b l \cdot r \\ m_{22} &= m_b l^2 + I_{by} \\ I_{bl} &= I_{bz} + m_b l^2 \\ G_b &= m_b g \cdot l \\ m_{31} &= 2I_{wd} + \frac{2b^2}{r^2}(I_{wa} + m_w r^2) \end{aligned} \tag{6}$$

The torques vector of the vehicle is defined as

$$\tau = [(u_r + u_l), -(u_r + u_l), \tfrac{b}{r}(u_r - u_l)]^T \tag{7}$$

Thus, by defining $u_1 = u_r + u_l$ and $u_2 = u_r - u_l$, the torques vector of the robotic vehicle is written as

$$\tau = [u_1, -u_1, u_2]^T \tag{8}$$

https://doi.org/10.1017/S0263574719000456 Published online by Cambridge University Press

After intermediate computations, the dynamic model of the pendulum is written also in the affine-in-the-input form:[1,2]

$$\begin{pmatrix} \ddot{\psi} \\ \ddot{\theta} \\ \ddot{\alpha} \end{pmatrix} = \begin{pmatrix} f_1 \\ f_2 \\ f_3 \end{pmatrix} + \begin{pmatrix} g_1 & 0 \\ g_2 & 0 \\ 0 & g_3 \end{pmatrix} \begin{pmatrix} u_1 \\ u_2 \end{pmatrix} \tag{9}$$

or by defining the state vector $[x_1, x_2, x_3, x_4, x_5, x_6]^T = [\psi, \dot{\psi}, \theta, \dot{\theta}, \alpha, \dot{\alpha}]^T$ it can be written in the form:

$$\begin{pmatrix} \dot{x}_1 \\ \dot{x}_2 \\ \dot{x}_3 \\ \dot{x}_4 \\ \dot{x}_5 \\ \dot{x}_6 \end{pmatrix} = \begin{pmatrix} x_2 \\ f_1 \\ x_4 \\ f_2 \\ x_6 \\ f_3 \end{pmatrix} + \begin{pmatrix} 0 & 0 \\ g_1 & 0 \\ 0 & 0 \\ g_2 & 0 \\ 0 & 0 \\ 0 & g_3 \end{pmatrix} \begin{pmatrix} u_1 \\ u_2 \end{pmatrix} \tag{10}$$

where

$$\begin{aligned} f_1 = \Delta_1^{-1}\{&m_{12}m_{22}sin(\theta)(\dot{\theta}^2 + \dot{\alpha}^2) \\ &-m_{12}I_{bl}sin(\theta)cos^2(\theta)\dot{\alpha}^2 - m_{12}G_b sin(\theta)cos(\theta) \\ &+2(m_{22} + m_{12}cos(\theta))D_b(\dot{\theta} - \dot{\psi}) - 2m_{22}D_w\dot{\psi}\} \end{aligned} \tag{11}$$

$$\Rightarrow f_1 = \frac{\tilde{f}_1}{\Delta_1}$$

$$\begin{gathered} g_1 = \Delta_1^{-1}\{m_{22} + m_{12}cos(\theta)\} \\ \Rightarrow g_1 = \tfrac{\tilde{g}_1}{\Delta_1} \end{gathered} \tag{12}$$

$$\Delta_1 = m_{11}m_{22} - m_{12}^2cos^2(\theta) \tag{13}$$

Additionally, it holds that

$$\begin{aligned} f_2 = \Delta_1^{-1}\{&m_{11}I_{bl}sin(\theta)cos(\theta)\dot{\alpha}^2 + m_{11}G_b sin(\theta) \\ &-m_{12}^2sin(\theta)cos(\theta)(\dot{\theta}^2 + \dot{\alpha}^2) \\ &-2(m_{11} + m_{12}cos(\theta))D_b(\dot{\theta} - \dot{\psi}) + 2m_{12}cos(\theta)D_w\dot{\psi})\} \end{aligned} \tag{14}$$

$$\Rightarrow f_2 = \frac{\tilde{f}_2}{\Delta_1}$$

$$\begin{gathered} g_2 = \Delta_2^{-1}\{-m_{11} + m_{12}cos(\theta)\} \\ \Rightarrow g_2 = \tfrac{\tilde{g}_2}{\Delta_2} \end{gathered} \tag{15}$$

$$\Delta_2 = m_{33} - I_{bl}sin^2(\theta) \tag{16}$$

Moreover, it holds that

$$\begin{aligned} f_3 = \Delta_2^{-1}\{&-2I_{bl}sin(\theta)cos(\theta)\dot{\theta}\dot{\alpha} - m_{12}sin(\theta)\dot{\psi}\dot{\alpha} \\ &-\tfrac{2b^2}{r^2}(D_b + D_w)\dot{\alpha}\} \end{aligned} \tag{17}$$

$$\begin{gathered} g_3 = \Delta_2^{-1}\left\{\tfrac{b}{r}\right\} \\ \Rightarrow g_3 = \tfrac{\tilde{g}_3}{\Delta_2} \end{gathered} \tag{18}$$

https://doi.org/10.1017/S0263574719000456 Published online by Cambridge University Press

3. Approximate Linearization of the WIP Model

The system of the WIP is linearized around a temporary operating point (equilibrium) which is defined as (x^*, u^*), where x^* is the present value of the system's state vector and u^* is the last value of the control input vector that was applied to it. The linearized description of the system is

$$\dot{x} = Ax + Bu + \tilde{d} \tag{19}$$

where matrices A and B are defined as

$$A = \nabla_x f(x) + \nabla_x g_A(x) u_1 + \nabla_x g_B(x) u_2 \tag{20}$$

Using the previous states-space description, one gets that

$$B = [g_A(x)\ g_B(x)] = \begin{pmatrix} 0 & 0 \\ g_1 & 0 \\ 0 & 0 \\ g_2 & 0 \\ 0 & 0 \\ 0 & g_3 \end{pmatrix} \tag{21}$$

The Jacobian matrix $\nabla_x f(x)$ has the following form:

$$\nabla_x f(x) = \begin{pmatrix} 0 & 1 & 0 & 0 & 0 & 0 \\ \frac{\partial f_1}{\partial x_1} & \frac{\partial f_1}{\partial x_2} & \frac{\partial f_1}{\partial x_3} & \frac{\partial f_1}{\partial x_4} & \frac{\partial f_1}{\partial x_5} & \frac{\partial f_1}{\partial x_6} \\ 0 & 0 & 0 & 1 & 0 & 0 \\ \frac{\partial f_2}{\partial x_1} & \frac{\partial f_2}{\partial x_2} & \frac{\partial f_2}{\partial x_3} & \frac{\partial f_2}{\partial x_4} & \frac{\partial f_2}{\partial x_5} & \frac{\partial f_2}{\partial x_6} \\ 0 & 0 & 0 & 0 & 0 & 1 \\ \frac{\partial f_3}{\partial x_1} & \frac{\partial f_3}{\partial x_2} & \frac{\partial f_3}{\partial x_3} & \frac{\partial f_3}{\partial x_4} & \frac{\partial f_3}{\partial x_5} & \frac{\partial f_3}{\partial x_6} \end{pmatrix} \tag{22}$$

To compute the elements of the above Jacobian matrix, one proceeds as follows:

$$\frac{\partial \tilde{f}_1}{\partial x_1} = 0 \tag{23}$$

$$\frac{\partial \tilde{f}_1}{\partial x_2} = -2m_{12}D_w - 2(m_{22} + m_{12}cos(x_3))D_b \tag{24}$$

$$\begin{aligned} \frac{\partial \tilde{f}_1}{\partial x_3} = {} & m_{12}m_{22}cos(x_3)(x_4^2 + x_6^2) - m_{12}I_{bl}[cos^3(x_3) - 2sin^2(x_3)cos(x_3)]x_6^2 \\ & -m_{12}G_b[cos^2(x_3) - sin^2(x_3)] - 2m_{12}sin(x_3)D_b(x_4 - x_2) \end{aligned} \tag{25}$$

$$\frac{\partial \tilde{f}_1}{\partial x_4} = 2m_{12}m_{22}sin(x_3)x_4 + 2(m_{22} + m_{12}cos(x_3))D_b \tag{26}$$

$$\frac{\partial \tilde{f}_1}{\partial x_5} = 0 \tag{27}$$

$$\frac{\partial \tilde{f}_1}{\partial x_6} = 2m_{12}m_{22}sin(x_3)x_6 - 2m_{12}I_{bl}sin(x_3)cos^2(x_3)x_6 \tag{28}$$

In a similar manner, one finds

$$\frac{\partial \tilde{f}_2}{\partial x_1} = 0 \tag{29}$$

$$\frac{\partial \tilde{f}_2}{\partial x_2} = 2(m_{11} + m_{12}cos(x_3))D_b + 2m_{12}cos(x_3)D_w \tag{30}$$

$$\begin{aligned} \frac{\partial \tilde{f}_2}{\partial x_3} = {} & m_{11}I_{bl}[cos^2(x_3) - sin(x_3)]x_6^2 - m_{11}G_b cos(x_3) \\ & -m_{12}^2[cos(x_3) - sin^2(x_3)](x_4^2 + x_6^2) \\ & +2m_{12}sin(x_3)D_b(x_4 - x_2) - 2m_{12}sin(x_3)D_w x_2 \end{aligned} \tag{31}$$

https://doi.org/10.1017/S0263574719000456 Published online by Cambridge University Press

$$\frac{\partial \tilde{f}_2}{\partial x_4} = -m_{12}^2 sin(x_3)cos(x_3)2x_4 - 2[m_{11} + m_{12}cos(x_3)]D_b \tag{32}$$

$$\frac{\partial \tilde{f}_2}{\partial x_5} = 0 \tag{33}$$

$$\frac{\partial \tilde{f}_2}{\partial x_5} = m_{11} I_{bl} sin(x_3)cos(x_3)2x_6 - m_{12}^2 sin(x_3)cos(x_3)2x_6 \tag{34}$$

Equivalently, one finds that

$$\frac{\partial \tilde{f}_3}{\partial x_1} = 0 \tag{35}$$

$$\frac{\partial \tilde{f}_3}{\partial x_2} = -m_{12} sin(x_3)x_6 \tag{36}$$

$$\frac{\partial \tilde{f}_3}{\partial x_3} = -2I_{bl}[cos^2(x_3) - sin^2(x_3)]x_4 x_6 - m_{12}cos(x_3)x_2 x_6 \tag{37}$$

$$\frac{\partial \tilde{f}_3}{\partial x_4} = -2I_{bl} sin(x_3)cos(x_3)x_6 \tag{38}$$

$$\frac{\partial \tilde{f}_3}{\partial x_5} = 0 \tag{39}$$

$$\frac{\partial \tilde{f}_3}{\partial x_6} = -2I_{bl} sin(x_3)cos(x_3)x_4 - m_{12} sin(x_3)x_2 - \frac{2b^2}{r^2}(D_b + D_w) \tag{40}$$

Following a similar procedure, one finds that $\frac{\partial \tilde{g}_1}{\partial x_1} = 0$, $\frac{\partial \tilde{g}_1}{\partial x_2} = 0$, $\frac{\partial \tilde{g}_1}{\partial x_3} = -m_{12} sin(x_3)$, $\frac{\partial \tilde{g}_1}{\partial x_4} = 0$, $\frac{\partial \tilde{g}_1}{\partial x_5} = 0$, $\frac{\partial \tilde{g}_1}{\partial x_6} = 0$.

Additionally, one gets that $\frac{\partial \tilde{g}_2}{\partial x_1} = 0$, $\frac{\partial \tilde{g}_2}{\partial x_2} = 0$, $\frac{\partial \tilde{g}_2}{\partial x_3} = 2I_{bl} sin(x_3)cos(x_3)$, $\frac{\partial \tilde{g}_2}{\partial x_4} = 0$, $\frac{\partial \tilde{g}_2}{\partial x_5} = 0$, $\frac{\partial \tilde{g}_2}{\partial x_6} = 0$.

Equivalently, one obtains $\frac{\partial \tilde{g}_3}{\partial x_1} = 0$, $\frac{\partial \tilde{g}_3}{\partial x_2} = 0$, $\frac{\partial \tilde{g}_3}{\partial x_3} = 0$, $\frac{\partial \tilde{g}_3}{\partial x_4} = 0$, $\frac{\partial \tilde{g}_3}{\partial x_5} = 0$, $\frac{\partial \tilde{g}_3}{\partial x_6} = 0$.

Following a similar procedure, one finds $\frac{\partial \Delta_1}{\partial x_1} = 0$, $\frac{\partial \Delta_1}{\partial x_2} = 0$, $\frac{\partial \Delta_1}{\partial x_3} = m_{12}^2 sin(x_3)$, $\frac{\partial \Delta_1}{\partial x_4} = 0$, $\frac{\partial \Delta_1}{\partial x_5} = 0$, $\frac{\partial \Delta_1}{\partial x_6} = 0$.

Equivalently, one finds $\frac{\partial \Delta_2}{\partial x_1} = 0$, $\frac{\partial \Delta_2}{\partial x_2} = 0$, $\frac{\partial \Delta_2}{\partial x_3} = 2I_{bl} sin(x_3)cos(x_3)$, $\frac{\partial \Delta_2}{\partial x_4} = 0$, $\frac{\partial \Delta_2}{\partial x_5} = 0$, $\frac{\partial \Delta_2}{\partial x_6} = 0$.

About the elements of the second row of the Jacobian matrix $\nabla_x f(x)$ and for $j = 1, 2, \ldots, 6$, it holds that

$$\frac{\partial f_1}{\partial x_j} = \frac{\frac{\partial \tilde{f}_1}{\partial x_j}\Delta_1 - \tilde{f}_1 \frac{\partial \Delta_1}{\partial x_j}}{\Delta_1^2} \tag{41}$$

About the elements of the fourth row of the Jacobian matrix $\nabla_x f(x)$ and for $j = 1, 2, \ldots, 6$, it holds that

$$\frac{\partial f_2}{\partial x_j} = \frac{\frac{\partial \tilde{f}_2}{\partial x_j}\Delta_1 - \tilde{f}_2 \frac{\partial \Delta_1}{\partial x_j}}{\Delta_1^2} \tag{42}$$

About the elements of the sixth row of the Jacobian matrix $\nabla_x f(x)$ and for $j = 1, 2, \ldots, 6$, it holds that

$$\frac{\partial f_3}{\partial x_j} = \frac{\frac{\partial \tilde{f}_3}{\partial x_j}\Delta_2 - \tilde{f}_3 \frac{\partial \Delta_2}{\partial x_j}}{\Delta_2^2} \tag{43}$$

https://doi.org/10.1017/S0263574719000456 Published online by Cambridge University Press

About the Jacobian matrix $\nabla_x g_A$, one has that

$$\nabla_x g_A(x) = \begin{pmatrix} 0 & 0 & 0 & 0 & 0 & 0 \\ \frac{\partial g_1}{\partial x_1} & \frac{\partial g_1}{\partial x_2} & \frac{\partial g_1}{\partial x_3} & \frac{\partial g_1}{\partial x_4} & \frac{\partial g_1}{\partial x_5} & \frac{\partial g_1}{\partial x_6} \\ 0 & 0 & 0 & 0 & 0 & 0 \\ \frac{\partial g_2}{\partial x_1} & \frac{\partial g_2}{\partial x_2} & \frac{\partial g_2}{\partial x_3} & \frac{\partial g_2}{\partial x_4} & \frac{\partial g_2}{\partial x_5} & \frac{\partial g_2}{\partial x_6} \\ 0 & 0 & 0 & 0 & 0 & 0 \\ 0 & 0 & 0 & 0 & 0 & 0 \end{pmatrix} \tag{44}$$

About the elements of the second row of the Jacobian matrix $\nabla_x g_A$ and for $j = 1, 2, \ldots, 6$, it holds that

$$\frac{\partial g_1}{\partial x_j} = \frac{\frac{\partial \tilde{g}_1}{\partial x_j}\Delta_1 - \tilde{g}_1 \frac{\partial \Delta_1}{\partial x_j}}{\Delta_1^2} \tag{45}$$

About the elements of the fourth row of the Jacobian matrix $\nabla_x g_A$ and for $j = 1, 2, \ldots, 6$, it holds that

$$\frac{\partial g_2}{\partial x_j} = \frac{\frac{\partial \tilde{g}_2}{\partial x_j}\Delta_2 - \tilde{g}_2 \frac{\partial \Delta_2}{\partial x_j}}{\Delta_2^2} \tag{46}$$

About the Jacobian matrix $\nabla_x g_B$, one has that

$$\nabla_x g_B(x) = \begin{pmatrix} 0 & 0 & 0 & 0 & 0 & 0 \\ 0 & 0 & 0 & 0 & 0 & 0 \\ 0 & 0 & 0 & 0 & 0 & 0 \\ 0 & 0 & 0 & 0 & 0 & 0 \\ 0 & 0 & 0 & 0 & 0 & 0 \\ \frac{\partial g_3}{\partial x_1} & \frac{\partial g_3}{\partial x_2} & \frac{\partial g_3}{\partial x_3} & \frac{\partial g_3}{\partial x_4} & \frac{\partial g_3}{\partial x_5} & \frac{\partial g_3}{\partial x_6} \end{pmatrix} \tag{47}$$

About the elements of the sixth row of the Jacobian matrix $\nabla_x g_B(x)$ and for $j = 1, 2, \ldots, 6$, it holds that

$$\frac{\partial g_3}{\partial x_j} = \frac{\frac{\partial \tilde{g}_3}{\partial x_j}\Delta_2 - \tilde{g}_3 \frac{\partial \Delta_2}{\partial x_j}}{\Delta_1^2} \tag{48}$$

It is possible to include the actuators' dynamics (DC motors) in the state-space model of the WIP. This would only increase the dimensionality of the state-space description but would not modify at all the application of the control method. The stages of implementation of the nonlinear optimal control approach remain unaltered and arrive at the solution of an algebraic Riccati equation with matrices of elevated dimensionality too. The control inputs of the model, previously standing for the torques generated by the DC motors, are now substituted by the voltages applied to the field windings of the motors. Alternatively, one can consider the control of the wheeled robotic system in successive loops. In the inner loop, one finds the control inputs of the mobile robot, which are the torques of the DC motors. Next, these control inputs become reference setpoints for the outer loop, which are controlled by the voltages applied to the field windings of the DC motors. Using Lyapunov stability analysis, one can prove again the global asymptotic stability for the control loop for the extended state-space model.

4. Design of an H-infinity Nonlinear Feedback Controller

4.1. Equivalent linearized dynamics of the WIP

After linearization around its current operating point, the dynamic model for the WIP is written as

$$\dot{x} = Ax + Bu + d_1 \tag{49}$$

Parameter d_1 stands for the linearization error in wheeled pendulum's model appearing in Eq. (49). The reference setpoints for the state vector of the aforementioned dynamic model are denoted by $x_d = [x_1^d, \ldots, x_6^d]^T$. Tracking of this trajectory is succeeded after applying the control input u^*. At every time instant, the control input u^* is assumed to differ from the control input u appearing in Eq.

https://doi.org/10.1017/S0263574719000456 Published online by Cambridge University Press

(49) by an amount equal to Δu, that is, $u^* = u + \Delta u$

$$\dot{x}_d = Ax_d + Bu^* + d_2 \tag{50}$$

The dynamics of the controlled system described in Eq. (49) can be also written as

$$\dot{x} = Ax + Bu + Bu^* - Bu^* + d_1 \tag{51}$$

and by denoting $d_3 = -Bu^* + d_1$ as an aggregate disturbance term, one obtains

$$\dot{x} = Ax + Bu + Bu^* + d_3 \tag{52}$$

By subtracting Eq. (50) from Eq. (52), one has

$$\dot{x} - \dot{x}_d = A(x - x_d) + Bu + d_3 - d_2 \tag{53}$$

denoting the tracking error as $e = x - x_d$ and the aggregate disturbance term as $\tilde{d} = d_3 - d_2$, the tracking error dynamics becomes

$$\dot{e} = Ae + Bu + \tilde{d} \tag{54}$$

The above linearized form of the robot's model can be efficiently controlled after applying an H-infinity feedback control scheme.

4.2. The nonlinear H-infinity control

The initial nonlinear model of WIP is in the form

$$\dot{x} = f(x, u) \;\; x \in R^n, \;\; u \in R^m \tag{55}$$

Linearization of the model of the WIP is performed at each iteration of the control algorithm round its present operating point $(x^*, u^*) = (x(t), u(t - T_s))$. The linearized equivalent of the system is described by

$$\dot{x} = Ax + Bu + L\tilde{d} \;\; x \in R^n, \;\; u \in R^m, \;\; \tilde{d} \in R^q \tag{56}$$

where matrices A and B are obtained from the computation of the previously defined Jacobians and vector $\tilde{d}$ denotes disturbance terms due to linearization errors. The problem of disturbance rejection for the linearized model that is described by

$$\begin{aligned} \dot{x} &= Ax + Bu + L\tilde{d} \\ y &= Cx \end{aligned} \tag{57}$$

where $x \in R^n$, $u \in R^m$, $\tilde{d} \in R^q$, and $y \in R^p$, cannot be handled efficiently if the classical LQR control scheme is applied. This is because of the existence of the perturbation term $\tilde{d}$. The disturbance term $\tilde{d}$ apart from modeling (parametric) uncertainty and external perturbation terms can also represent noise terms of any distribution.

In the H_∞ control approach, a feedback control scheme is designed for trajectory tracking by the system's state vector and simultaneous disturbance rejection, considering that the disturbance affects the system in the worst possible manner. The disturbances' effects are incorporated in the following quadratic cost function:

$$J(t) = \tfrac{1}{2}\int_0^T [y^T(t)y(t) + ru^T(t)u(t) - \rho^2 \tilde{d}^T(t)\tilde{d}(t)]dt, \quad r, \rho > 0 \tag{58}$$

The significance of the negative sign in the cost function's term that is associated with the perturbation variable $\tilde{d}(t)$ is that the disturbance tries to maximize the cost function $J(t)$ while the control signal $u(t)$ tries to minimize it. The physical meaning of the relation given above is that the control signal and the disturbances compete to each other within a min–max differential game. This problem of min–max optimization can be written as

$$min_u max_{\tilde{d}} J(u, \tilde{d}) \tag{59}$$

The objective of the optimization procedure is to compute a control signal $u(t)$ which can compensate for the worst possible disturbance, that is, externally imposed to WIP. However, the solution to the

https://doi.org/10.1017/S0263574719000456 Published online by Cambridge University Press

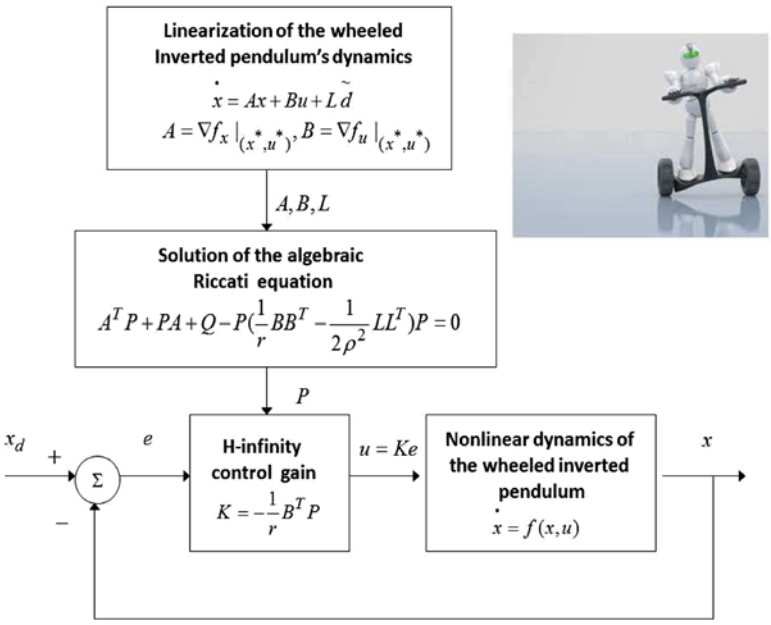

Fig. 2. Diagram of the control scheme for the underactuated WIP.

min–max optimization problem is directly related to the value of the parameter ρ. This means that there is an upper bound in the disturbances magnitude that can be annihilated by the control signal.

4.3. Computation of the feedback control gains

For the linearized system given by Eq. (57), the cost function of Eq. (58) is defined, where the coefficient r determines the penalization of the control input and the weight coefficient ρ determines the reward of the disturbances' effects. It is assumed that (i) the energy that is transferred from the disturbances signal $\tilde{d}(t)$ is bounded, that is, $\int_0^\infty \tilde{d}^T(t)\tilde{d}(t)dt < \infty$, (ii) matrices $[A, B]$ and $[A, L]$ are stabilizable, and (iii) matrix $[A, C]$ is detectable. Then, the optimal feedback control law is given by

$$u(t) = -Kx(t) \tag{60}$$

with $K = \frac{1}{r}B^T P$, where P is a positive definite symmetric matrix which is obtained from the solution of the Riccati equation

$$A^T P + PA + Q - P\left(\tfrac{1}{r}BB^T - \tfrac{1}{2\rho^2}LL^T\right)P = 0 \tag{61}$$

where Q is also a positive semi-definite symmetric matrix. The worst case disturbance is given by

$$\tilde{d}(t) = \tfrac{1}{\rho^2}L^T Px(t) \tag{62}$$

The diagram of the considered control loop for the WIP is depicted in Fig. 2.

4.4. Riccati equation coefficients in H-infinity control robustness

Parameter ρ in Eq. (58) is an indication of the closed-loop system robustness. If the values of $\rho > 0$ are excessively decreased with respect to r, then the solution of the Riccati equation is no longer a positive definite matrix. Consequently, there is a lower bound ρ_{min} of ρ for which the H_∞ control problem has a solution. The acceptable values of ρ lie in the interval $[\rho_{min}, \infty)$. If ρ_{min} is found and used in the design of the H_∞ controller, then the closed-loop system will have increased robustness. Unlike this, if a value $\rho > \rho_{min}$ is used, then an admissible stabilizing H_∞ controller will be derived but it will be a suboptimal one. The Hamiltonian matrix

$$H = \begin{pmatrix} A & -\left(\frac{1}{r}BB^T - \frac{1}{\rho^2}LL^T\right) \\ -Q & -A^T \end{pmatrix} \tag{63}$$

https://doi.org/10.1017/S0263574719000456 Published online by Cambridge University Press

provides a criterion for the existence of a solution of the Riccati equation (Eq. (61)). A necessary condition for the solution of the algebraic Riccati equation to be a positive definite symmetric matrix is that H has no imaginary eigenvalues.[23]

5. Lyapunov Stability Analysis

Through Lyapunov stability analysis, it will be shown that the proposed nonlinear control scheme assures H_∞ tracking performance for the underactuated WIP, and that in the case of bounded disturbance terms, asymptotic convergence to the reference setpoints is succeeded. The tracking error dynamics for the WIP is written in the form:

$$\dot{e} = Ae + Bu + L\tilde{d} \tag{64}$$

where in the wheeled pendulum's case, $L = I \in R^6$ with I being the identity matrix. Variable $\tilde{d}$ denotes model uncertainties and external disturbances of the wheeled pendulum's model. The following Lyapunov equation is considered:

$$V = \tfrac{1}{2} e^T P e \tag{65}$$

where $e = x - x_d$ is the tracking error. By differentiating with respect to time, one obtains

$$\begin{gathered} \dot{V} = \tfrac{1}{2}\dot{e}^T P e + \tfrac{1}{2} e P \dot{e} \Rightarrow \\ \dot{V} = \tfrac{1}{2}[Ae + Bu + L\tilde{d}]^T P e + \tfrac{1}{2} e^T P [Ae + Bu + L\tilde{d}] \Rightarrow \end{gathered} \tag{66}$$

$$\begin{gathered} \dot{V} = \tfrac{1}{2}[e^T A^T + u^T B^T + \tilde{d}^T L^T] P e \\ + \tfrac{1}{2} e^T P [Ae + Bu + L\tilde{d}] \Rightarrow \end{gathered} \tag{67}$$

$$\begin{gathered} \dot{V} = \tfrac{1}{2} e^T A^T P e + \tfrac{1}{2} u^T B^T P e + \tfrac{1}{2} \tilde{d}^T L^T P e \\ + \tfrac{1}{2} e^T P A e + \tfrac{1}{2} e^T P B u + \tfrac{1}{2} e^T P L \tilde{d} \end{gathered} \tag{68}$$

The previous equation is rewritten as

$$\begin{gathered} \dot{V} = \tfrac{1}{2} e^T (A^T P + P A) e + \left(\tfrac{1}{2} u^T B^T P e + \tfrac{1}{2} e^T P B u\right) \\ + \left(\tfrac{1}{2} \tilde{d}^T L^T P e + \tfrac{1}{2} e^T P L \tilde{d}\right) \end{gathered} \tag{69}$$

Assumption: For given positive definite matrix Q and coefficients r and ρ, there exists a positive definite matrix P, which is the solution of the following matrix equation:

$$A^T P + P A = -Q + P\left(\tfrac{2}{r} B B^T - \tfrac{1}{\rho^2} L L^T\right) P \tag{70}$$

Moreover, the following feedback control law is applied to the system:

$$u = -\tfrac{1}{r} B^T P e \tag{71}$$

By substituting Eqs. (70) and (71), one obtains

$$\begin{gathered} \dot{V} = \tfrac{1}{2} e^T \left[-Q + P\left(\tfrac{2}{r} B B^T - \tfrac{1}{\rho^2} L L^T\right) P \right] e \\ + e^T P B \left(-\tfrac{1}{r} B^T P e \right) + e^T P L \tilde{d} \Rightarrow \end{gathered} \tag{72}$$

$$\begin{gathered} \dot{V} = -\tfrac{1}{2} e^T Q e + \tfrac{1}{r} e^T P B B^T P e - \tfrac{1}{2\rho^2} e^T P L L^T P e \\ - \tfrac{1}{r} e^T P B B^T P e + e^T P L \tilde{d} \end{gathered} \tag{73}$$

which after intermediate operations gives

$$\dot{V} = -\tfrac{1}{2} e^T Q e - \tfrac{1}{2\rho^2} e^T P L L^T P e + e^T P L \tilde{d} \tag{74}$$

or, equivalently

$$\begin{gathered} \dot{V} = -\tfrac{1}{2} e^T Q e - \tfrac{1}{2\rho^2} e^T P L L^T P e \\ + \tfrac{1}{2} e^T P L \tilde{d} + \tfrac{1}{2} \tilde{d}^T L^T P e \end{gathered} \tag{75}$$

https://doi.org/10.1017/S0263574719000456 Published online by Cambridge University Press

Lemma: The following inequality holds:

$$\tfrac{1}{2}e^T L\tilde{d} + \tfrac{1}{2}\tilde{d}L^T Pe - \tfrac{1}{2\rho^2}e^T PLL^T Pe \leq \tfrac{1}{2}\rho^2\tilde{d}^T\tilde{d} \tag{76}$$

Proof: The binomial $(\rho\alpha - \frac{1}{\rho}b)^2$ is considered. Expanding the left part of the above inequality, one gets

$$\begin{gathered}\rho^2a^2 + \tfrac{1}{\rho^2}b^2 - 2ab \geq 0 \Rightarrow \tfrac{1}{2}\rho^2a^2 + \tfrac{1}{2\rho^2}b^2 - ab \geq 0 \Rightarrow \\ ab - \tfrac{1}{2\rho^2}b^2 \leq \tfrac{1}{2}\rho^2a^2 \Rightarrow \tfrac{1}{2}ab + \tfrac{1}{2}ab - \tfrac{1}{2\rho^2}b^2 \leq \tfrac{1}{2}\rho^2a^2\end{gathered} \tag{77}$$

The following substitutions are carried out: $a = \tilde{d}$ and $b = e^T PL$ and the previous relation becomes

$$\tfrac{1}{2}\tilde{d}^T L^T Pe + \tfrac{1}{2}e^T PL\tilde{d} - \tfrac{1}{2\rho^2}e^T PLL^T Pe \leq \tfrac{1}{2}\rho^2\tilde{d}^T\tilde{d} \tag{78}$$

Equation (78) is substituted in Eq. (75) and the inequality is enforced, thus giving

$$\dot{V} \leq -\tfrac{1}{2}e^T Qe + \tfrac{1}{2}\rho^2\tilde{d}^T\tilde{d} \tag{79}$$

Equation (79) shows that the H_∞ tracking performance criterion is satisfied. The integration of $\dot{V}$ from 0 to T gives

$$\begin{gathered}\int_0^T \dot{V}(t)dt \leq -\tfrac{1}{2}\int_0^T ||e||_Q^2 dt + \tfrac{1}{2}\rho^2\int_0^T ||\tilde{d}||^2 dt \Rightarrow \\ 2V(T) + \int_0^T ||e||_Q^2 dt \leq 2V(0) + \rho^2\int_0^T ||\tilde{d}||^2 dt\end{gathered} \tag{80}$$

Moreover, if there exists a positive constant $M_d > 0$ such that

$$\int_0^\infty ||\tilde{d}||^2 dt \leq M_d \tag{81}$$

then, one gets

$$\int_0^\infty ||e||_Q^2 dt \leq 2V(0) + \rho^2 M_d \tag{82}$$

Thus, the integral $\int_0^\infty ||e||_Q^2 dt$ is bounded. Moreover, $V(T)$ is bounded and from the definition of the Lyapunov function V in Eq. (65), it becomes clear that $e(t)$ will be also bounded since $e(t) \in \Omega_e = \{e | e^T Pe \leq 2V(0) + \rho^2 M_d\}$. According to the above and with the use of Barbalat's Lemma, one obtains $\lim_{t\to\infty} e(t) = 0$.

The outline of the global stability proof is that at each iteration of the control algorithm, the state vector of the WIP converges towards the temporary equilibrium and the temporary equilibrium, in turn, converges towards the reference trajectory. Thus, the control scheme exhibits global asymptotic stability properties and not local stability. Assume the ith iteration of the control algorithm and the ith time interval about which a positive definite symmetric matrix P is obtained from the solution of the Riccati equation appearing in Eq. (70). By following the stages of the stability proof, one arrives at Eq. (79) which shows that the H-infinity tracking performance criterion holds. By selecting the attenuation coefficient ρ to be sufficiently small and, in particular, to satisfy $\rho^2 < ||e||_Q^2 / ||\tilde{d}||^2$ one has that the first derivative of the Lyapunov function is upper bounded by 0. Therefore, for the ith time interval, it is proven that the Lyapunov function defined in Eq. (65) is a decreasing one. This signifies that between the beginning and the end of the ith time interval, there will be a drop of the value of the Lyapunov function and since matrix P is a positive definite one, the only way for this to happen is the Euclidean norm of the state vector error e to be decreasing. This means that comparing to the beginning of each time interval, the distance of the state vector error from 0 at the end of the time interval has diminished. Consequently, as the iterations of the control algorithm advance the tracking error will approach zero, and this is a global asymptotic stability condition.

Remark 1: The dynamics of the physical system under control, that is, of the WIP, is a continuous-time one. To simulate the robotic system's dynamics, the related state-space model undergoes discretization following common discretization methods, such as finite difference methods (Euler approximations). The computation of the optimal (H-infinity) control input essentially relies on a continuous-time algebraic Riccati equation. This Riccati equation is repetitively solved at each

https://doi.org/10.1017/S0263574719000456 Published online by Cambridge University Press

sampling period of the control algorithm after using the approximately linearized state-space representation of the system in continuous time. Consequently, the dynamics of the robotic system is a continuous-time one, so is the computation of the optimal control input. However, the computer-based implementation of the control method uses the sampled discrete-time representation of the robotic system's dynamics and the sampled discrete-time values of the control inputs. The time step used for the numerical integration of robotic system's dynamics and the sampling period of the control inputs are the same. Within one sampling period, the control input remains as computed from the solution of the aforementioned Riccati equation; therefore, it can be said that the control input is kept constant between two consecutive time steps of the control algorithm.

Remark 2: The presented control method is of global asymptotic stability. Although, the concept for linearization of dynamical system around fixed equilibria with the use of Taylor series expansion is an established one, the approach for linearizing the dynamics of a system around time-varying equilibria, that is, operating points which are updated at each sampling period, is a novel one. Actually, there are rolling operating points which are recomputed at each time step of the control method, and which comprise the present value of the state vector of the robotic system and the last value of the control inputs vector that was applied to it. Furthermore, the solution of the optimal control problem for the linearized model of the system, taking place at each sampling period, relies on a the solution of a novel algebraic Riccati equation. Thus, a Riccati equation has been selected so as to assure that (i) the H-infinity tracking performance criterion will be reached in the Lyapunov stability analysis of the control system and (ii) the control loop will be globally asymptotically stable. The provided stability analysis does not overlook the effects of modelling errors which are due to the approximate linearization of the robotic system. On the contrary, such perturbation terms are taken into account and are shown to be asymptotically compensated by the robustness of the control algorithm.

6. Robust State Estimation with the Use of the H_∞ Kalman Filter

The control loop has to be implemented with the use of information provided by a small number of sensors and by processing only a small number of state variables. To reconstruct the missing information about the state vector of the WIP, it is proposed to use a filtering scheme and based on it to apply state estimation-based control.[24] The recursion of the H_∞ Kalman Filter, for the model of the WIP, can be formulated in terms of a *measurement update* and a *time update* part

Measurement update:

$$\begin{aligned} D(k) &= [I - \theta W(k) P^-(k) + C^T(k) R(k)^{-1} C(k) P^-(k)]^{-1} \\ K(k) &= P^-(k) D(k) C^T(k) R(k)^{-1} \\ \hat{x}(k) &= \hat{x}^-(k) + K(k)[y(k) - C\hat{x}^-(k)] \end{aligned} \tag{83}$$

Time update:

$$\begin{aligned} \hat{x}^-(k+1) &= A(k)x(k) + B(k)u(k) \\ P^-(k+1) &= A(k) P^-(k) D(k) A^T(k) + Q(k) \end{aligned} \tag{84}$$

where it is assumed that parameter θ is sufficiently small to assure that the covariance matrix $P^-(k)^{-1} - \theta W(k) + C^T(k) R(k)^{-1} C(k)$ will be positive definite. When $\theta = 0$, the H_∞ Kalman Filter becomes equivalent to the standard Kalman Filter. One can measure only a part of the state vector of the WIP (for instance, state variables x_1, x_3, and x_5) and can estimate through filtering the rest of the state vector elements. Moreover, the proposed Kalman filtering method can be used for sensor fusion purposes.

7. Simulation Tests

The performance of the nonlinear optimal (H-infinity) control method for the problem of control and stabilization of the WIP is demonstrated through simulation experiments. The reference path that the two-wheel vehicle followed in the simulation experiments is shown in Figs. 3 and 4. The results about the convergence of the state variables of the wheeled pendulum $x_i,\ i = 1, \ldots, 6$ to their reference setpoints, as well as the results about the variation of the control inputs $u_i,\ i = 1, 2$, are depicted in Figs. 5–12. It can be observed that under the proposed control scheme, fast and accurate tracking is achieved for the elements of the state vector of the WIP. Moreover, it is shown that the variations of the control input remain moderate and smooth.

https://doi.org/10.1017/S0263574719000456 Published online by Cambridge University Press

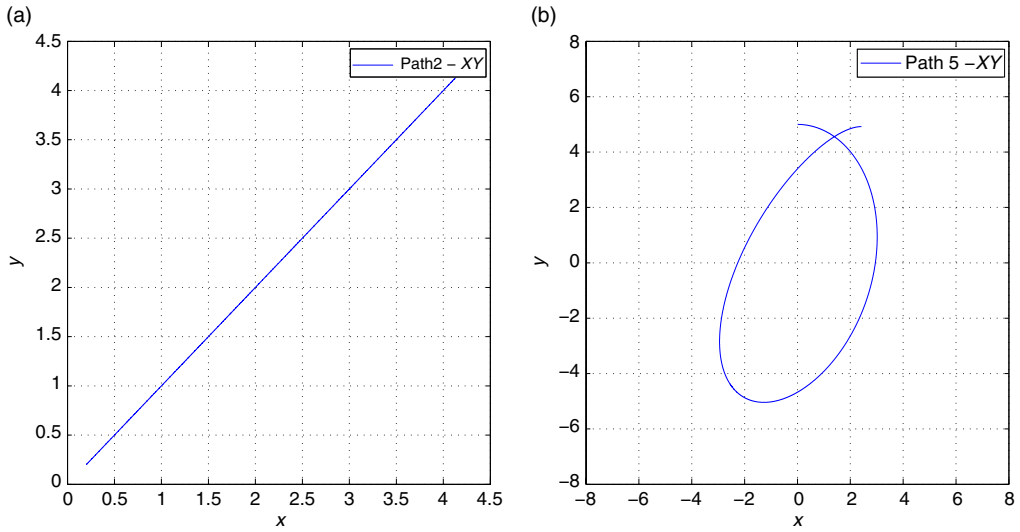

Fig. 3. Trajectory on the xy plane, followed by the wheel pendulum (a) in the case of test 1 and (b) in the case of test 2.

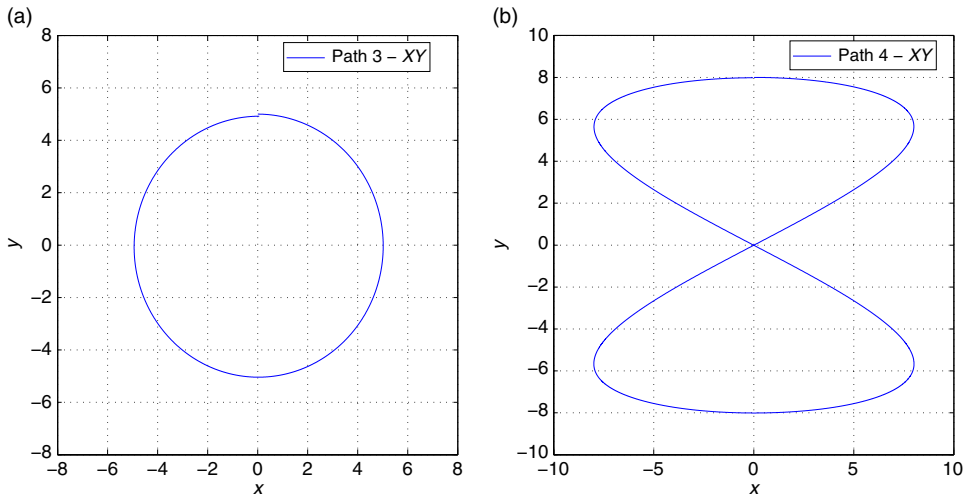

Fig. 4. Trajectory on the xy plane, followed by the wheel pendulum (a) in the case of test 3 and (b) in the case of test 4.

The necessary and sufficient condition for the implementation of the proposed control method is the existence of a solution for the algebraic Riccati equation given in Eq. (70). The transient performance of the control loop depends on the selection of the values of parameters r, ρ, and Q in the aforementioned Riccati equation. To perform state estimation-based feedback control for the WIP, through the measurement of a small number of its state vector elements, the H-infinity Kalman Filter has been used as a robust state estimator. In the simulation diagrams, the real values of the state vector elements are plotted in blue, the estimated values are printed in green, and the associated reference setpoints are depicted in red.

Despite its conceptual and computational simplicity, the proposed control method performs equally well to global linearization-based control methods and to Lyapunov theory-based control schemes. The advantages of the nonlinear optimal (H-infinity) control approach for the model of the WIP are outlined as follows; (a) the optimal control scheme avoids the elaborated state variables transformations (diffeomorphisms) which are met in global linearization-based control approaches, (b) in the optimal control method, the control inputs are exerted directly on the initial nonlinear dynamic model of the wheeled pendulum and not on its linearized equivalent description. In such a

https://doi.org/10.1017/S0263574719000456 Published online by Cambridge University Press

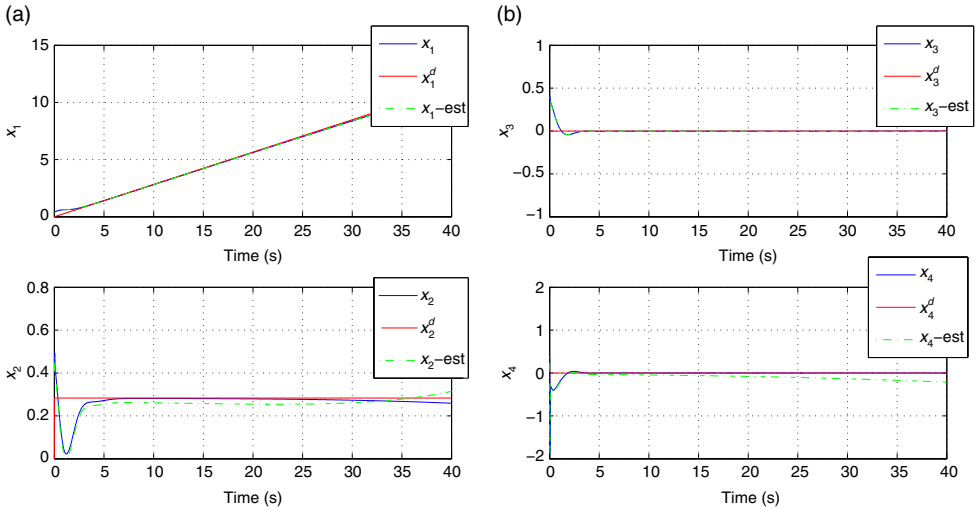

Fig. 5. Test 1: (a) convergence of state variables x_1 and x_2 of the WIP to their reference setpoints and (b) convergence of state variables x_3 and x_4 of the WIP to their reference setpoints.

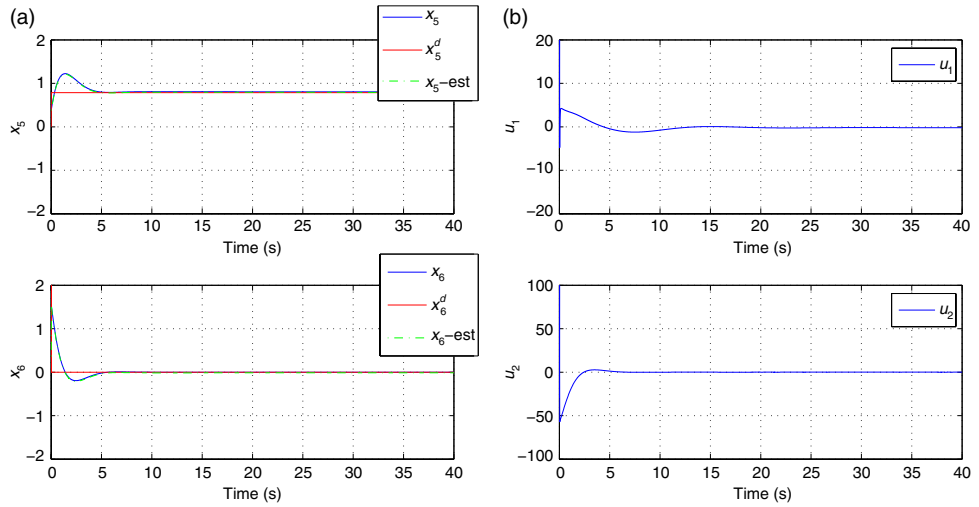

Fig. 6. Test 1: (a) convergence of state variables x_5 and x_6 of the WIP to their reference setpoints and (b) control inputs u_1 and u_2 provided by the wheels' actuators.

manner, inverse transformations and the related singularities problems are avoided, and (c) the proposed control method retains the main features of linear optimal control, that is, accurate tracking of the reference trajectories under smooth and moderate variations of the control inputs.

The control inputs of the wheeled-pendulum system which are depicted in Fig. 8(b)–10(b) can be implemented in real DC-actuators. Actually, the magnitude of the control inputs, which are the torques provided by the motors to the robotic system, remain moderate. Consequently, it can be assured that for the autonomous navigation of the robotic system, even in the case of following complicated reference paths, the control inputs change smoothly and saturation of the actuators is avoided, Regarding the programming of the controller, this can take place with the pulse width modulation technique. The values of gains r, ρ and of matrix Q which appear in the algebraic Riccati equation of the control loop have been changed so as to achieve the satisfactory transients of the control system.

Remark 3: The objective of the proposed nonlinear optimal (H-infinity) control method is (i) to achieve accurate and fast tracking of reference setpoints for all state variables of the considered model of the WIP, (ii) to keep moderate the variations of the control inputs, thus also assuring minimum energy consumption by the actuators of the robotic vehicle. The solution of the nonlinear optimal control problem for mobile robots can raise significantly their level of autonomy. By reducing energy

https://doi.org/10.1017/S0263574719000456 Published online by Cambridge University Press

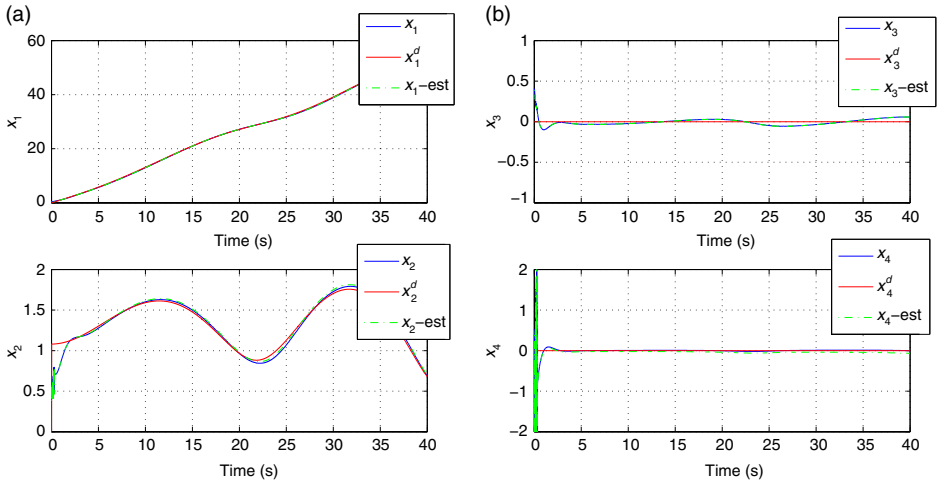

Fig. 7. Test 2: (a) convergence of state variables x_1 and x_2 of the WIP to their reference setpoints (b) convergence of state variables x_3 and x_4 of the WIP to their reference setpoints.

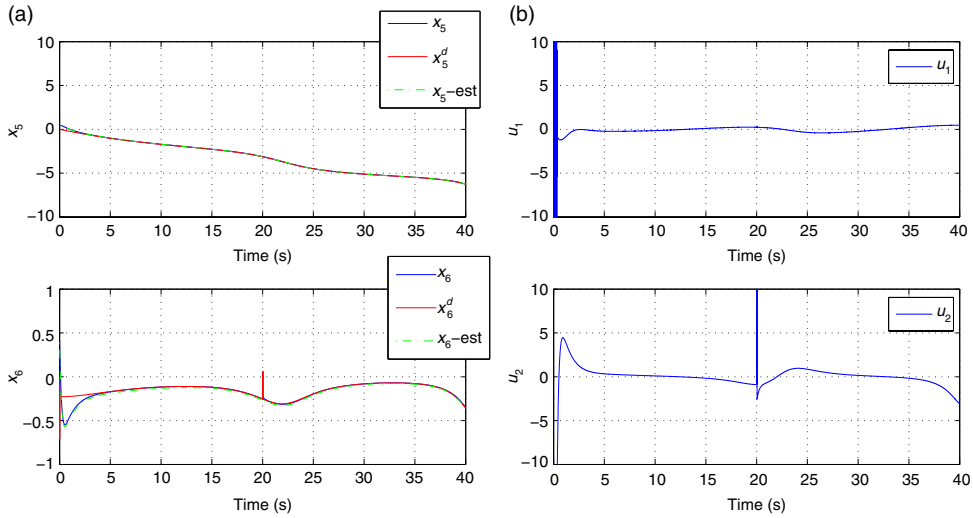

Fig. 8. Test 2: (a) convergence of state variables x_5 and x_6 of the WIP to their reference setpoints and (b) control inputs u_1 and u_2 provided by the wheels' actuators.

consumption by the robot's actuators, the vehicle's stay in recharging lots becomes less frequent and its operational capacity is also increased. Considering that the WIP is primarily used in patrolling and security tasks, as well as in the transportation of individuals, it can be inferred that through the article's control method such robots can remain functional for prolonged time periods. Besides, by implementing control through reduced consumption of energy, the discharge of the robotic vehicle's batteries is slowed down and their lifetime is also prolonged.

Remark 4: Functioning of the robot's actuators beyond their torque and power limits is unlikely to take place if optimal control schemes are implemented. This is because optimal control assures moderate variations for the robot's control inputs. Besides, optimal control avoids abrupt variations in the control signals and thus high-frequency components in the control inputs are unlikely to appear. In particular, about the control input signals that appear in the aforementioned diagrams, what is noted as high-frequency components can be avoided by suitable tuning of the parameters appearing in the algebraic Riccati equation that is solved for computing the control inputs. The transient performance of the controller depends on the gains r and ρ and on matrix Q. The smallest value of ρ for which the Riccati equation can be solved is the one that provides maximum robustness to the control loop of the WIP.

https://doi.org/10.1017/S0263574719000456 Published online by Cambridge University Press

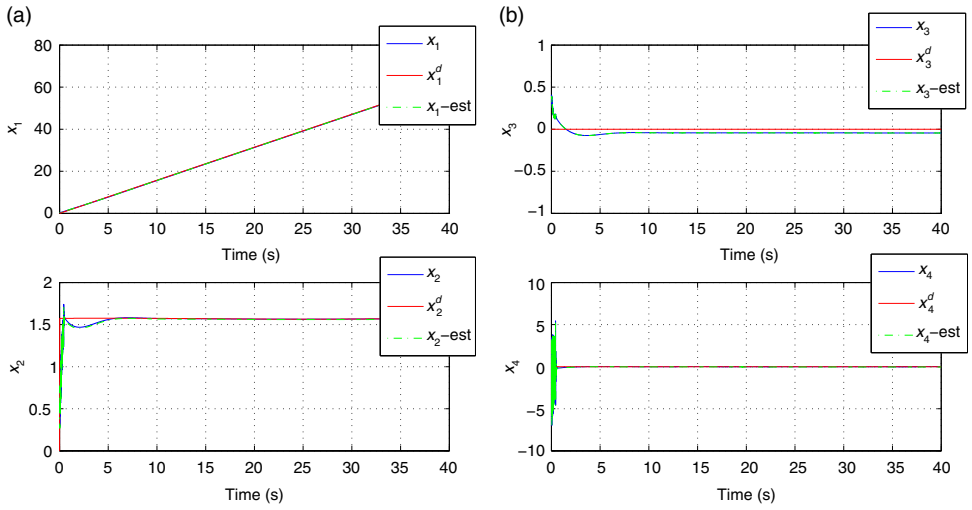

Fig. 9. Test 3: (a) convergence of state variables x_1 and x_2 of the WIP to their reference setpoints and (b) convergence of state variables x_3 and x_4 of the WIP to their reference setpoints.

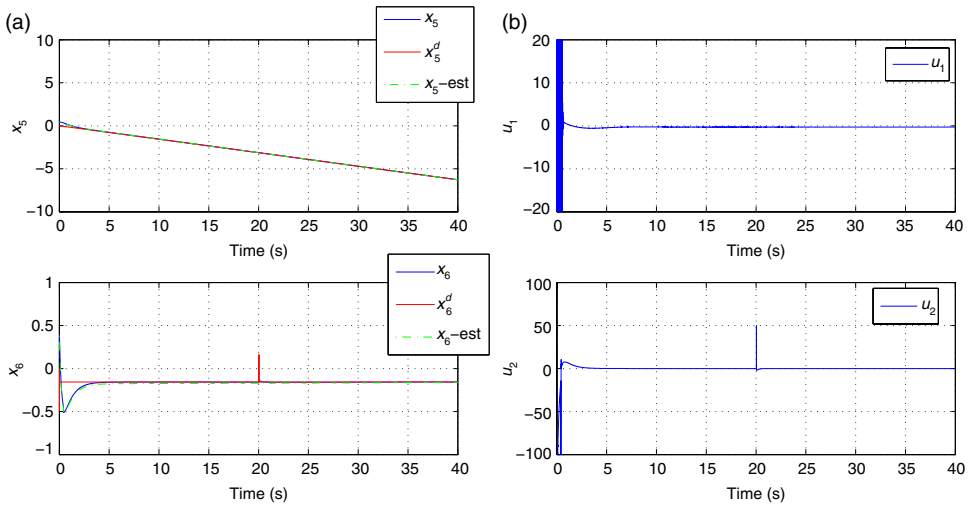

Fig. 10. Test 3: (a) convergence of state variables x_5 and x_6 of the WIP to their reference setpoints and (b) control inputs u_1 and u_2 provided by the wheels' actuators.

8. Conclusions

The article proposes a nonlinear optimal (H-infinity) control method for the dynamic model of the WIP. The control of such a robotic system exhibits elevated difficulty due to underactuation and strong nonlinearities in its dynamic model. The dynamic model of the wheeled pendulum undergoes first approximate linearization around a temporary operating point which is recomputed at each time step of the control method. The linearization procedure makes use of Taylor series expansion and requires the computation of the associated Jacobian matrices. For the approximately linearized model of the wheeled pendulum, the optimal (H-infinity) feedback control problem is solved.

Actually, the proposed H-infinity controller stands for the solution of the optimal control problem for the model of the wheeled pendulum, under model uncertainties and external perturbations. The computation of the controller's feedback gains requires the repetitive solution of an algebraic Riccati equation which takes place at each iteration of the control algorithm. The stability properties of the control scheme are proven with the use of Lyapunov analysis. First, it is demonstrated that the control loop satisfies the H-infinity tracking performance criterion. Moreover, under moderate conditions, it is proven that the control loop is globally asymptotically stable. Finally, by using the H-infinity Kalman Filter as a robust observer, it is shown that a state estimation-based feedback control scheme can be implemented.

https://doi.org/10.1017/S0263574719000456 Published online by Cambridge University Press

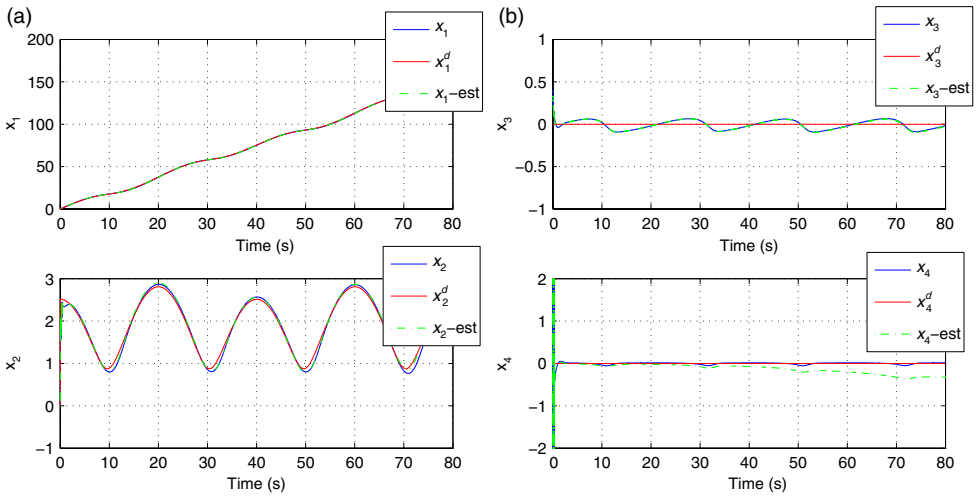

Fig. 11. Test 4: (a) convergence of state variables x_1 and x_2 of the WIP to their reference setpoints and (b) convergence of state variables x_3 and x_4 of the WIP to their reference setpoints.

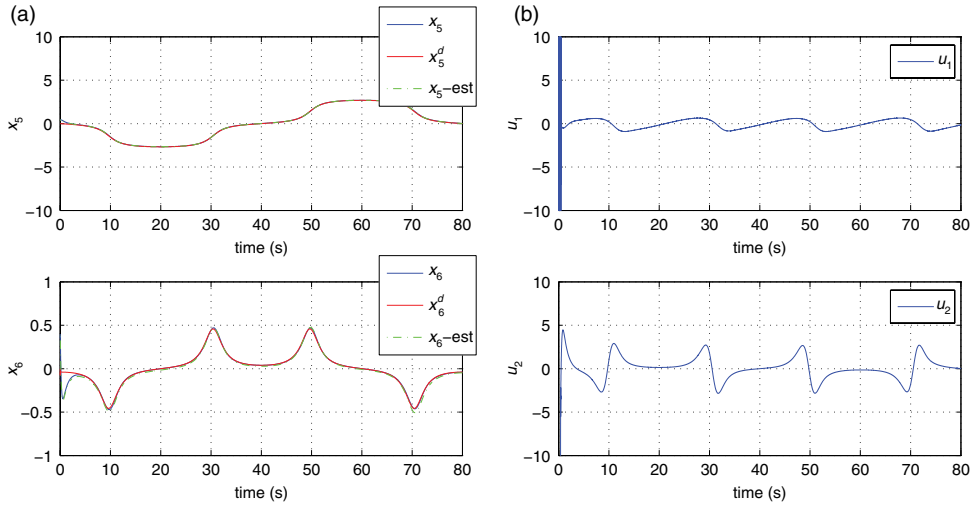

Fig. 12. Test 4: (a) convergence of state variables x_5 and x_6 of the WIP to their reference setpoints and (b) control inputs u_1 and u_2 provided by the wheels' actuators.

Acknowledgments

This work has been part of the 2016–2019 Research Cooperation Agreement between the Industrial Systems Institute (Unit of Industrial Automation) and the University of Northumbria (Nonlinear Control Group) under the title "Nonlinear Control and Filtering."

References

1. J. Huang, S. Ri, L. Liu, Y. Wang, J. Kim and G. Rek, "Nonlinear disturbance observer-based dynamic surface control of mobile wheeled inverted pendulum," *IEEE Trans. Control Syst. Technol.* **23**(6), 2400–2407 (2015).
2. S. Ri, J. Huang, C. Tao, M. Ri, Y. Ri and D. Han, "A High-Order Disturbance Observer Based Sliding Mode Velocity Control of Mobile Wheeled Inverted Pendulum Systems," *IEEE 12th International World Congress on Intelligent Contorl and Automation, IEEE WCICA 2016*, Guilin, China (2014, June).
3. K. Yosida, M. Sekikawa and K. Hosomi, "Nonlinear analysis on purely mechanical stabilization of a wheeled inverted pendulum on a slope," *Nonlinear Dyn.* **83**(1–2), 905–917 (2016).
4. K. Yokoyama and M. Takahashi, "Dynamics-based nonlinear acceleration control and energy shaping for a mobile inverted pendulum with a slider mechanism," *IEEE Trans. Control Syst. Technol.* **24**(1), 40–55 (2016).
5. Z. Li and C. Yang, "Neural-adaptive output feedback control of a class of transportation vehicles based on wheeled inverted pendulum models," *IEEE Trans. Control Syst. Technol.* **20**(6), 1583–1591 (2012).

https://doi.org/10.1017/S0263574719000456 Published online by Cambridge University Press

6. T. Tokei, R. Imamura and S. Yuta, "Baggage transportation and navigation by a wheeled inverted pendulum mobile robot," *IEEE Trans. Ind. Electron.* **56**(10), 3985–3994 (2009).
7. K. Pathak, J. Franch and S. K. Agrawal, "Velocity and position control of a wheeled inverted pendulum by partial feedback linearization," *IEEE Trans. Rob.* **21**(3), 505–513 (2005).
8. R. M. Brissila and V. Sankarannarayanan, "Nonlinear control of mobile inverted pendulum," *Rob. Auton. Syst.* **70**, 145–155 (2015).
9. H. Fukushima, M. Kakue, K. Kon and F. Matsuno, "Transformation control of an inverted pendulum for a mobile robot with wheel-arms using partial feedback linearization and polytopic model set," *IEEE Trans. Rob.* **23**(3), 774–783 (2013).
10. V. Maralidharan and A. D. Mahindrakar, "Position stabilization and waypoint tracking control of mobile inverted pendulum robot," *IEEE Trans. Control Syst. Technol.* **22**(6), 2360–2367 (2014).
11. J. Y. Xu, Z. G. Guo and T. H. Lee, "Design and implementation of integral sliding-mode control on an underactuated two-wheeled mobile robot," *IEEE Trans. Ind. Electron.* **61**(7), 3671–3681 (2014).
12. J. Huang, F. Ding, T. Fukuda, and T. Matsuno, "Modelling and velocity control for a novel narrow vehicle based on mobile wheeled inverted pendulum," *IEEE Trans. Control Syst. Technol.* **21**(5), 1607–1617 (2013).
13. J. Huang, Z. H. Guan, T. Matsuno, T. Fukuda and K. Sekiyama, "Sliding-mode velocity control of mobile-wheeled inverted-pendulum systems," *IEEE Trans. Rob.* **26**(4), 750–758 (2010).
14. F. Dai, X. Gao, S. Jiang, W. Guo and Y. Liu, "A two-wheeled inverted pendulum robot with friction compensation," *Mechatronics* **30**, 116–125 (2015).
15. Y. Zhou and Z. Wang, "Motion controller design of wheeled inverted pendulum with an input delay via optimal control theory," *J. Optim. Theory Appl.* **138**(2), 625–645 (2016).
16. C. Yang, Z. Li, R. Cui and B. Xu, "Neural network-based motion control of underactuated wheeled inverted pendulum models," *IEEE Trans. Neural Networks Learn. Syst.* **25**(11), 2004–2016 (2014).
17. C. C. Tsai, H. C. Huang and S. C. Lin, "Adaptive neural network control of a self-balancing two-wheeled scooter," *IEEE Trans. Ind. Electron.* **57**(4), 1420–1428 (2010).
18. M. T. Ravichandran and A. D. Mahindrakar, "Robust stabilization of a class of underactuated mechanical systems using time-scaling and Lyapunov redesign," *IEEE Trans. Ind. Electron.* **58**(3), 4299–4213 (2011).
19. Z. Li and J. Luo, "Adaptive robust dynamic balance and motion controls of mobile wheeled inverted pendulums," *IEEE Trans. Control Syst. Technol.* **17**(1), 233–241 (2009).
20. W. Ye, Z. Li, C. Yang, J. Sun, C. Y. Su and R. Lu, "Vision-based human tracking control of a wheeled inverted pendulum robot," *IEEE Trans. Cybern.* **46**(1), 2423–2434 (2016).
21. M. Yue, S. Wang and J. Z. Sun, "Simultaneous balancing and trajectory tracking control for two-wheeled inverted pendulum vehicles: a composite control approach," *Neurocomputing* **101**, 44–54 (2016).
22. M. Yue, C. An, Y. Du and J. Sun, "Indirect adaptive fuzzy control for a nonholonomic/underactuated wheeled inverted pendulum vehicle based on a data-driven trajectory planning," *Fuzzy Sets Syst.* **290**, 158–177 (2016).
23. G. Rigatos, "Modelling and Control for Intelligent Industrial Systems," **In:** *Adaptive Algorithms in Robotics and Industrial Engineering* (Springer, Berlin, Heidelberg, 2011).
24. G. Rigatos, *Nonlinear Control and Filtering Using Differential Flatness Approaches: Applications to Electromechanicsl Systems* (Springer, Switzerland, 2015).
25. G. Rigatos, *Intelligent Renewable Energy systems: Modelling and Control* (Springer, Switzerland, 2017).
26. G. Rigatos, P. Siano and C. Cecati, "A new nonlinear H-infinity feedback control approach for three-phase voltage source converters," *Electr. Power Compon. Syst.* **44**(3), 302–312 (2015).
27. G. G. Rigatos and S. G. Tzafestas, "Extended Kalman filtering for fuzzy modelling and multi-sensor fusion," *Math. Comput. Modell. Dyn. Syst.* **13**, 251–266 (2007).
28. M. Basseville and I. Nikiforov, *Detection of Abrupt Changes: Theory and Applications* (Prentice-Hall, Upper Saddle River, New Jersey, USA, 1993).
29. G. Rigatos and Q. Zhang, "Fuzzy model validation using the local statistical approach," *Fuzzy Sets Syst.* **60**(7), 882–904 (2009).
30. G. J. Toussaint, T. Basar and F. Bullo, "H_∞ Optimal Tracking Control Techniques for Nonlinear Underactuated Systems," *Proceedings of IEEE CDC 2000, 39th IEEE Conference on Decision and Control*, Sydney, Australia (2000, December).
31. L. Lublin and M. Athans, "An Experimental Comparison of and Designs for Interferometer Testbed," **In**: *Feedback Control, Nonlinear Systems and Complexity* (B. Francis and A. Tannenbaum, eds.) (Springer, Berlin, Heidelberg, 1995) pp. 150–172.
32. B. P. Gibbs, *Advanced Kalman Filtering, Least Squares and Modelling: A Practical Handbook* (J. Wiley, Hoboken, New Jersey, USA, 2011).
33. D. Simon, "A game theory approach to constrained minimax state estimation," *IEEE Trans. Signal Process.* **54**(2), 405–412 (2006).
34. Z. J. Wang and F. C. Wang, "The Development and Control of a Two-Wheeled Inverted Pendulum," *Proceedings of the IEEE SICE 2017 International Conference*, Kanazawa, Japan (2017, September).
35. K. S. Phogat, R. Banavar and D. Chatterjee, "Structure Preserving Discrete-Time Optimal Maneuvers of a Wheeled Inverted Pendulum," *6th IFAC Workshop on Lagrangian and Hamiltonian Methods for Nonlinear Control LHMNC 2018*, Valparaiso, Chile (2018, May).
36. J. Huang, M. Ri, D. Wu and S. Ri, "Interval type-2 fuzzy logic modeling and control of a mobile two-wheeled inverted pendulum," *IEEE Trans. Fuzzy Syst.* **26**(4), 2039–2038 (2018).

37. M. Yue, C. An, and Z. Li, "Constrained adaptive robust trajectory tracking for WIP vehicles using model predictive control and extended state observer," *IEEE Trans. Syst. Man Cybern.* **48**(5), 733–742 (2018).
38. E. Sihite and T. Bewley, "Attitude Estimation of a High-Yaw-Rate Mobile Inverted Pendulum; Comparison of Extended Kalman Filtering, Complementary Filtering, and Motion Capture," *IEEE ACC 2018, Annual American Control Conference (ACC)* Wisconsin Center, Milwaukee, USA (2018, June).
39. Y. Zhang, L. Zhang, W. Wang, Y. Li and Q. Zhang, "Design and implementation of a two-wheel and hopping robot with a linkage mechanism," *IEEE Access* **6**, 42422–42430 (2018).
40. A. Weiss, E. Hadida and U. B. Hanan, "Optimizing step climbing by two connected wheeled inverted pendulum models," *Procedia Manuf.* **21**, 236–242 (2018).
41. S. Han and J. M. Lee, "Balancing and velocity control of a unicycle robot based on the dynamic," *IEEE Trans. Ind. Electron.* **68**(1), 405–413 (2015).
42. F. Dai, X. Gao, S. Jiang, W. Guo and Y. Liu, "A two-wheeled inverted pendulum robot with friction compensation," *Mechatronics* **30**, 116–125 (2015).

https://doi.org/10.1017/S0263574719000456 Published online by Cambridge University Press